Front. Phys. China, 2008, 3(2): 113–125
DOI 10.1007/s11467-008-0024-0

REVIEW ARTICLE

Xiong-jun LIU, Xin LIU, Leong-Chuan KWEK, Choo Hiap OH

Manipulating atomic states via optical orbital angular-momentum

Abstract Optical orbital angular-momentum (OAM) has more complex mechanics than the spin degree of photons, and may have a broad range of application. Manipulating atomic states via OAM has become an interesting topic. In this paper, we first review the general theory of generating adiabatic gauge field in ultracold atomic systems by coupling atoms to external optical fields with OAM, and point out the applications of the generated adiabatic gauge field. Then, we review our work in this field, including the generation of macroscopic superposition of vortex-antivortex states and spin Hall effect (SHE) in cold atoms.

Keywords orbital angular momentum, adiabatic Gauge field, vortex states, spin Hall effect, quantum state transfer, ultracold atoms

PACS numbers 32.80.Qk, 32.80.Pj, 03.65.Vf, 03.75.Kk, 72.25.Fe, 72.25.Hg

1 Introduction

Coherent optical control of the quantum state of atoms is the most important task in quantum optics and atomic physics, in terms of the application to quantum information science and discovering the basic features of quantum many-body physics. A direct control of atomic quantum states can be achieved by transferring the external optical information to atoms via atom-light interaction [1−19]. The technique of quantum state transfer between photons and atoms has vital importance in the practical quantum information technologies. As a result, developing appropriate techniques for coherent transfer of quantum states between photons and atoms has become one of the central topics of quantum information science and been widely studied in both theory and experiment in recent years. The elegant schemes of this field include, e.g. the coherent control of single-atom by high-Q cavity QED [1−5], and the quantum state transfer between photons and an ensemble of atoms through electromagnetically induced transparency (EIT) [6−22]. The applications of coherent manipulation of atomic quantum states are now widely investigated in quantum memory, quantum computing, and quantum teleportation [23−28].

On the other hand, it has been widely acknowledged that ultracold atomic gases have become an ideal playground to experimentally investigate many-body physics [29]. The remarkable controllability in the parameters of these systems allows a clean study of complexr physics in a controllable fashion. One of the most exciting advances in ultracold atomic gases is that rotating Bose-Einstein condensates (BECs) provide a conceptual link between the physics of trapped gases and the physics of condensed matter systems such as superfluids, type-II superconductors, and quantum-Hall effect (QHE) materials [30−36]. In the rotating BEC systems, the trap rotation provides an effective magnetic field for the electrically neutral atoms. For this, the Abrikosov lattice of quantized vortices [37] and the analog of the fractional

Xiong-jun LIU[1, 2], Xin LIU[2], Leong-Chuan KWEK[1, 3], Choo Hiap OH[1] (✉)

[1] Department of Physics, National University of Singapore, 2 Science Drive 3, Singapore 117542, Singapore
[2] Department of Physics, Texas A & M University, College Station, TX 77843-4242, USA
[3] National Institute of Education, Nanyang Technological University, 1 Nanyang Walk, Singapore 639798, Singapore
E-mail: phylx@physics.tamu.edu; phyohch@nus.edu.sg

Received March 4, 2008; accepted March 10, 2008

quantum Hall effect (FQHE) can be studied.

Recent advances in the optical coherent manipulation of ultracold atoms suggest an alternative to create adiabatic gauge fields for the atomic systems by coupling the atoms to external optical fields which are spatially dependent in the amplitude and phase [38−41], e.g. optical fields with orbital angular-momentum (OAM). Optical OAM has more complex mechanics than the spin degree of photons, and can have a broad range of application [42, 43]. The simplest class of light field carrying OAM is an optical vortex, which is a beam of light whose phase varies in a corkscrew-like manner along the beam's direction of propagation [45, 46]. The interacting Hamiltonian of atoms and optical field with OAM depends on the local spatial parameters, which results in an adiabatic gauge field for the motion of atoms under the adiabatic condition. Properly modifying the external optical fields yields different types of effective magnetic field, the curvature of the adiabatic gauge field. Different from the rotating BECs where only the constant and spin-independent effective magnetic field can be obtained [30], the effective magnetic field created using optical means has more freedom to be shaped and controlled, and then is very helpful to study new physics in ultracold atoms.

In this paper, we first review the basic idea of generating adiabatic gauge field in ultracold atomic system by coupling atoms to external optical fields with OAM, and point out the applications of the generated adiabatic gauge field. Then, we review our work in this field, including the generation of macroscopic superposition of vortex-antivortex states and spin Hall effect (SHE) in cold atoms.

The paper is organized as follows. In Section 2, we introduce the general discussion on the adiabatic gauge field for the ultracold atomic system; in Section 3, we give an example of the adiabatic gauge field in the three-level system; in Section 4, we discuss how to generate macroscopic superposition of vortex-antivortex states from a five-level M-type atomic system; in Section 5, we introduce an intriguing application of the created adiabatic gauge field: spin Hall effect in ultracold atoms; concluding remarks are given in Section 6.

2 Adiabatic gauge field in quantum system

2.1 Unitary transformation

The idea that adiabatic gauge fields can be generated in quantum systems was first proposed by Wilczek and Zee more than twenty years ago [47]. In this section, we shall review the general theory of the adiabatic gauge fields created in the quantum N-level systems. For convenience, we denote $H_0(r)$ as the unperturbed Hamiltonian that describes the N internal levels $|\chi_k\rangle (k = 1, 2, \cdots, N)$ for the system, and $\mathcal{E}_k$ as the eigenvalue of the corresponding energy level. In the presence of perturbation Hamiltonian H_I that can be created through e.g. external trap potentials, laser-induced coupling for atomic systems, etc., the dynamics of the quantum system can be studied via perturbation theory. Without loss of generality, in this paper we consider the case of a weak perturbation so that H_I does not induce the energy shift to the energy levels of internal Hamiltonian, but causes the coupling between different eigenstates $|\chi_k\rangle$. For this we can generally expand the wave function for the system according to $\tilde{\Psi}(\boldsymbol{r}, t) = \sum_{k=1}^{N} \Psi_k(\boldsymbol{r}) \exp(-\mathrm{i}\mathcal{E}_k t/\hbar)|\chi_k\rangle$, where $\mathcal{E}_k$ is the eigenvalue of the corresponding internal energy level. Denoting by $\Psi = (\Psi_1, \Psi_2, \cdots, \Psi_N)^{\mathrm{T}}$, the coupling between states Ψ_k by the interaction Hamiltonian can be given by

$$\mathrm{i}\hbar\frac{\partial \Psi}{\partial t} = \left[-\frac{\hbar^2}{2m}\nabla^2 + V(\boldsymbol{r})\right]\Psi + H_I(\boldsymbol{r})\Psi \tag{1}$$

where $V(\boldsymbol{r})$ is the external trap potential, and the interacting Hamiltonian H_I depends on the local parameters, e.g. the spatial position $\boldsymbol{r}$. The diagonalization of the interacting Hamiltonian can be done through a local unitary transformation $U(\boldsymbol{r})$,

$$\Psi = U(\boldsymbol{r})\Phi, \quad H_I^d = U^\dagger H_I U \tag{2}$$

where $\Phi = (\Phi_1, \Phi_2, \cdots, \Phi_N)$ is the diagonalized basis of the interacting Hamiltonian, and H_I^d is diagonal on this basis. The diagonal elements $(H_I^d)_{kk} = E_k$ represents the eigenvalue of Φ_k. Note that the specific form of the unitary transformation $U(\boldsymbol{r})$ shall be solely determined by the interacting Hamiltonian. Substituting the transformation (2) into Eq. (1) we obtain the equation of evolution for Φ that

$$\mathrm{i}\hbar\frac{\partial \Phi}{\partial t} = -\frac{\hbar^2}{2m}U^\dagger\nabla^2 U\Phi + U^\dagger V(\boldsymbol{r})U\Phi + H_I^d(\boldsymbol{r})\Phi \tag{3}$$

The form of the above equation can be simplified by introducing the gauge potential

$$\boldsymbol{A}(\boldsymbol{r}) = \mathrm{i}\frac{\hbar c}{e}U^\dagger(\boldsymbol{r})\nabla U(\boldsymbol{r}) \tag{4}$$

with e the electric charge constant.

Relying on the above definition of the gauge potential and after a straightforward calculation we find that the Eq. (3) can be rewritten as follows:

$$\mathrm{i}\hbar\frac{\partial \Phi}{\partial t} = \frac{1}{2m}\left[\mathrm{i}\hbar\nabla + \frac{e}{c}\boldsymbol{A}(\boldsymbol{r})\right]^2\Phi + V'(\boldsymbol{r})\Phi + H_I^d(\boldsymbol{r})\Phi \tag{5}$$

where $V' = U^\dagger V(\boldsymbol{r})U$. Since $U(\boldsymbol{r})$ considered here is a local unitary transformation on the N-dimensional Hilbert space, it is an $N \times N$ parameter-dependent matrix. As a result, the gauge defined based on Eq. (4) is non-Abelian and of the $N \times N$ matrix form (of the $SU(N)$ symmetry). The non-Abelian gauge field is associated with the curvature (effective magnetic field) that is given by

$$F_{\mu\nu} = \partial_\mu A_\nu - \partial_\nu A_\mu - \mathrm{i}\frac{e}{c}[A_\mu, A_\nu] \tag{6}$$

with the magnetic field $B_j = 1/2\epsilon_{jkl}F_{kl}$. One should keep in mind that to this step we do not apply the adiabatic condition in the equation of motion. The gauge field defined in Eq. (4) is a pure gauge and it is easy to verify that $F_{\mu\nu} = 0$. It is noteworthy that the non-Abelian pure gauge may have nontrivial significance by resulting in a phase to the wave function Φ:

$$\Phi(\boldsymbol{r}, t) \rightarrow \mathcal{P}\mathrm{e}^{\mathrm{i}\frac{e}{\hbar c}\int \boldsymbol{A}\cdot \mathrm{d}\boldsymbol{l}}\Phi(\boldsymbol{r}, t) \tag{7}$$

where $\mathcal{P}$ is the operator of chronological ordering. The above phase factor is known as Wilson loop integral [48]. This phase factor can be non-zero even for a pure gauge, since for the non-Abelian gauge field we have $\nabla \times \boldsymbol{A} \neq \boldsymbol{B} = 0$. To find the possible observable physics for this phase factor is an interesting issue in gauge field theory.

2.2 Adiabatic condition

In this paper, however, we are interested in the case that the adiabatic condition can be applied and then the adiabatic gauge field is obtained [49]. Under the adiabatic condition, the adiabatic gauge potential is generally associated with a non-zero curvature

$$F_{\mu\nu} \neq 0 \tag{8}$$

To have more sense of the adiabatic gauge field obtained above, we consider two special cases in the following.

First, let us suppose that the system is non-degenerate, i.e., E_n is different for different eigenstates Φ_n. Besides, the coupling between each two states, say Φ_j and Φ_k, induced by the off-diagonal element $\boldsymbol{A}_{jk}(\boldsymbol{r})$ satisfies

$$\left|\frac{\boldsymbol{P}\cdot \boldsymbol{A}_{jk}}{m(E_j - E_k)}\right| \ll 1 \tag{9}$$

the adiabatic condition is then approved and the transition between different states in Eq. (5) can be ignored. The non-Abelian gauge field is reduced from $SU(N)$ symmetry to N independent $U(1)$ Abelian gauge fields with

$$\begin{aligned}\boldsymbol{A}_j(\boldsymbol{r}) &= \mathrm{i}\frac{\hbar c}{e}(U^\dagger(\boldsymbol{r})\nabla U(\boldsymbol{r}))_{jj} \\ &= \mathrm{i}\hbar\langle \Phi_j|\nabla|\Phi_j\rangle, \quad j = 1, 2, \cdots, N\end{aligned} \tag{10}$$

and the corresponding scalar potential after applying the adiabatic condition:

$$\phi_j(\boldsymbol{r}) = \frac{1}{2m}\sum_{k\neq j}\boldsymbol{A}_{jk}\cdot \boldsymbol{A}_{kj}, \quad j = 1, 2, \cdots, N \tag{11}$$

In the dynamical equation of evolution (5), all components of the column vector Φ become decoupled to each other and now yield

$$\mathrm{i}\hbar\frac{\partial \Phi_j}{\partial t} = \frac{1}{2m}\left[\mathrm{i}\hbar\nabla + \frac{e}{c}\boldsymbol{A}_j(\boldsymbol{r})\right]^2\Phi_j + \bar{V}'_j(\boldsymbol{r})\Phi_j \tag{12}$$

with $V'_j(\boldsymbol{r}) = V'(\boldsymbol{r}) + \phi_j + E_j$. The curvature of $U(1)$ gauge fields is given by

$$F^{(j)}_{\mu\nu} = \partial_\mu A^{(j)}_\nu - \partial_\nu A^{(j)}_\mu \tag{13}$$

which is generally non-zero.

Another interesting possibility is that the system has degeneracy. Without loss of generality, we suppose Φ_1, $\Phi_2, \cdots, \Phi_m (m < N)$ consist of the degenerate subspace of the system, with energy eigenvalue E_g that differs from the eigenvalues of all remaining states. Similarly, when

$$\left|\frac{\boldsymbol{P}\cdot \boldsymbol{A}_{ij}}{m(E_g - E_j)}\right| \ll 1 \tag{14}$$

where $i = 1, 2, \cdots, m$ and $j = m+1, m+2, \cdots, N$. Then we denote reduced column vector $\Phi' = (\Phi_1, \Phi_2, \cdots, \Phi_m)^{\mathrm{T}}$, which satisfies the equation:

$$\mathrm{i}\hbar\frac{\partial \Phi'}{\partial t} = \frac{1}{2m}\left[\mathrm{i}\hbar\nabla + \frac{e}{c}\boldsymbol{A}'(\boldsymbol{r})\right]^2\Phi' + [V'(\boldsymbol{r}) + \phi' + E_g]\Phi' \tag{15}$$

where $\boldsymbol{A}'(\boldsymbol{r})$ is still non-diagonal $U(m)$ gauge field and $\boldsymbol{A}'_{jk}(\boldsymbol{r}) = \mathrm{i}\frac{\hbar c}{e}(U^\dagger(\boldsymbol{r})\nabla U(\boldsymbol{r}))_{jk}$. The scalar field ϕ' is also an $m \times m$ matrix with the elements $\phi'_{jk} = \frac{1}{2m}\sum_{l>m}\boldsymbol{A}_{jl}\cdot \boldsymbol{A}_{lk}$. The curvature can also be calculated with the Eq. (6), but now it is generally nonzero.

3 Example of adiabatic gauge field: three-level atomic system

As an example, in this section we calculate the adiabatic gauge field in the three-level Λ-type atomic system which couples to two external laser fields.

The three-level Λ-type system is shown in Fig. 1. The transition $|c\rangle \rightarrow |a\rangle$ is resonantly coupled by a pump field with the Rabi-frequency $\Omega_1 = \Omega_1^{(0)}\exp(\mathrm{i}\boldsymbol{k}_1\cdot\boldsymbol{r})$, where $\Omega_1^{(0)}(r)$ is the slowly spatially varying amplitude and $\boldsymbol{k}_1$ is the wave-vector. The probe field, whose Rabi frequency $\Omega_2 = \Omega_2^{(0)}(r)\mathrm{e}^{\mathrm{i}[\phi(\boldsymbol{r})+\boldsymbol{k}_2\cdot\boldsymbol{r}]}$ with $\Omega_2^{(0)}(r)$ the slowly spatially varying amplitude, couples resonantly the transition $|b\rangle \to |a\rangle$, where $\boldsymbol{k}_2$ is wave-vector of the probe field. $\phi(\boldsymbol{r})$ is the spatially-dependent phase. Defining the flip operators as $\hat{\sigma}_{\mu\nu} = |\mu\rangle\langle\nu|$ with the level indices $\mu,\nu = a,b,c$, the Hamiltonian in the present system reads

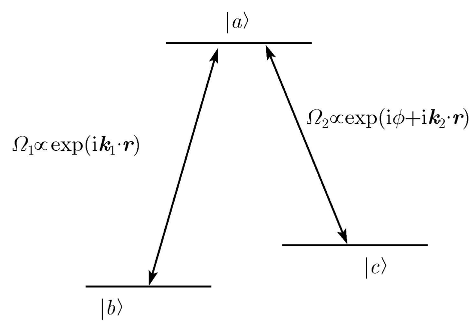

Fig. 1 Three-level Λ-type system couples to two external laser fields.

$$H = H_0 + H_I \tag{16}$$
$$H_0 = -\frac{\hbar^2}{2m_e}\nabla^2 + V(\boldsymbol{r})$$
$$H_I = -(\hbar\Omega_2\hat{\sigma}_{ab} + \hbar\Omega_1\hat{\sigma}_{ac}) + h.c.$$

where $V(\boldsymbol{r})$ is the external trap potential. To facilitate the subsequent discussion, H_0 is written in $\boldsymbol{r}$-representation other using flip operators in Eq. (16). The interaction Hamiltonian H_I can be diagonalized with the local unitary transformation: $\tilde{H}_I = U(\boldsymbol{r})H_IU^\dagger(\boldsymbol{r})$ with

$$U(\boldsymbol{r}) = \begin{pmatrix} \frac{1}{\sqrt{2}} & \frac{1}{\sqrt{2}}\sin\theta\mathrm{e}^{-\mathrm{i}S(\boldsymbol{r})} & \frac{1}{\sqrt{2}}\cos\theta \\ 0 & \cos\theta & -\sin\theta\mathrm{e}^{\mathrm{i}S(\boldsymbol{r})} \\ \frac{1}{\sqrt{2}} & -\frac{1}{\sqrt{2}}\sin\theta\mathrm{e}^{-\mathrm{i}S(\boldsymbol{r})} & -\frac{1}{\sqrt{2}}\cos\theta \end{pmatrix} \tag{17}$$

where $S = (\boldsymbol{k}_2 - \boldsymbol{k}_1)\cdot\boldsymbol{r} + \phi(\boldsymbol{r})$ and the mixing angle $\tan\theta(r) = |\Omega_2/\Omega_1|$. Under this unitary transformation, the three eigenstates of H_I are easily obtained as

$$|\Phi_+\rangle = \frac{1}{\sqrt{2}}(|a\rangle + \sin\theta\mathrm{e}^{-\mathrm{i}S(\boldsymbol{r})}|b\rangle + \cos\theta|c\rangle)$$
$$|\Phi_0\rangle = \cos\theta|b\rangle - \sin\theta\mathrm{e}^{\mathrm{i}S(\boldsymbol{r})}|c\rangle \tag{18}$$
$$|\Phi_-\rangle = \frac{1}{\sqrt{2}}(|a\rangle - \sin\theta\mathrm{e}^{-\mathrm{i}S(\boldsymbol{r})}|b\rangle - \cos\theta|c\rangle)$$

with the corresponding eigenvalues $E_\pm = \mp\frac{\hbar}{2}\Omega_0$ and $E_0 = 0$ where $\Omega_0 = \sqrt{|\Omega_1|^2 + |\Omega_2|^2}$. It is interesting that $|\Psi_0\rangle$, typically known as the dark state for a three-level Λ system [6, 7, 9, 10, 19–22], is a coherent superposition of two ground states, excluding the excited state. Dark state is also a central idea for the electromagnetically induced transparency (EIT), a prevailing modern technique in recent years to realize the slow light and quantum memory for photons [6–14].

According to the definition given in the previous section, by a straightforward calculation we find that the 3×3 matrix $\boldsymbol{A}$ in the three-level system has the following form:

$$\boldsymbol{A} = \frac{\hbar c}{\mathrm{e}}\begin{pmatrix} \frac{1}{\sqrt{2}}\sin^2\theta\nabla S & \left(\mathrm{i}\frac{1}{\sqrt{2}}\nabla\theta + \frac{1}{2\sqrt{2}}\sin2\theta\nabla S\right)\mathrm{e}^{-\mathrm{i}S} & -\frac{1}{\sqrt{2}}\sin^2\theta\nabla S \\ \left(-\mathrm{i}\frac{1}{\sqrt{2}}\nabla\theta + \frac{1}{2\sqrt{2}}\sin2\theta\nabla S\right)\mathrm{e}^{\mathrm{i}S} & -\sin^2\theta\nabla S & \left(\mathrm{i}\frac{1}{\sqrt{2}}\nabla\theta - \frac{1}{2\sqrt{2}}\sin2\theta\nabla S\right)\mathrm{e}^{\mathrm{i}S} \\ -\frac{1}{\sqrt{2}}\sin^2\theta\nabla S & \left(-\mathrm{i}\frac{1}{\sqrt{2}}\nabla\theta - \frac{1}{2\sqrt{2}}\sin2\theta\nabla S\right)\mathrm{e}^{-\mathrm{i}S} & \frac{1}{\sqrt{2}}\sin^2\theta\nabla S \end{pmatrix} \tag{19}$$

which generally is a $SU(3)$ non-Abelian gauge potential. Noting that the present system is non-degenerate, we have particular interest in the case when the adiabatic condition is satisfied. For this we require

$$\left|\frac{\boldsymbol{v}\cdot\boldsymbol{A}_{\alpha\beta}}{(E_\alpha - E_\beta)}\right| \ll 1, \quad \alpha \neq \beta = +,-,0 \tag{20}$$

which can be satisfied for sufficient large Rabi-frequency and small motion velocity. Under this condition we ignore the off diagonal elements of the gauge potential. A most interesting result can be achieved by applying the probe field with orbital angular momentum (OAM) $\hbar l$. In this way, the spatially-dependent phase of the probe field has the form: $\phi(\boldsymbol{r}) = l\arctan(y/x)$. Furthermore, we consider the special situation that the Rabi-frequency rate between the probe and pump fields satisfies $\left|\frac{\Omega_2}{\Omega_1}\right| = \lambda\rho \propto \rho$ with $\rho = \sqrt{x^2+y^2}$ the distance from z axis, and $|\Omega_2| \ll |\Omega_1|$, i.e., the probe field is much weaker than the pump field. The diagonal elements of gauge potential (19) follows the three constant effective magnetic fields

$$B^{++}=B^{--}=\hbar lc\lambda^2/e\hat{e}_z, \quad B^{00}=-2\hbar lc\lambda^2/e\hat{e}_z \quad (21)$$

This result clearly shows that atoms in the dark state ($|\Phi_0\rangle$) and in the bright states ($|\Phi_\pm\rangle$) experience the opposite magnetic fields, respectively in $+z$ and $-z$ direction. Such a situation will result in the different Landau-level structure for dark-state and bright-state particles (Fig. 2). If we further apply an effective electric field in say x direction, we can find atoms in $|\Phi_0\rangle$ move in the $+y$ direction, while the atoms in $|\Phi_\pm\rangle$ move in the $-y$ direction. This is in fact the basic idea in generating spin current in atoms [50, 51].

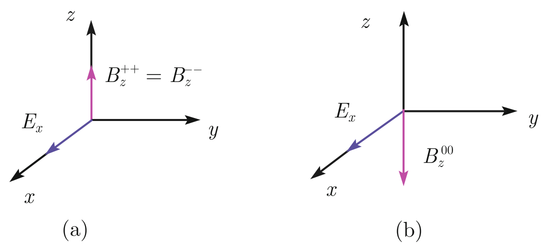

Fig. 2 Atoms in dark- and bright-states experience opposite effective magnetic fields but the same effective electric field.

An interesting extension from the above situation can be done by considering the four-level atomic tripod system [41], where there are three ground states. Two independent dark states in the tripod level configuration consist of the degenerate subspace of the system. According to our general discussion in Section 2, this will result in a $U(2)$ non-Abelian gauge field in the atomic adiabatic dynamics. The possibility of realization of monopole gauge field is also discussed in Ref. [41].

4 Generation of macroscopic superposition of vortex-antivortex states

By now we have shown that applying laser fields with OAM can generate effective magnetic fields for the orbital motion of atoms. This result can be understood as the coherent transfer of OAM between optical fields and atoms. A natural idea following this result is that one can generate atomic vortex states by transferring the optical vortex to atoms. As is well-known, in cold atoms such as Bose-Einstein condensates (BECs) in dilute gases, the stable existence of quantized vortices is one of the most striking and fascinating signatures of superfluidity [52]. Many works have been done on the nucleation of vortex lattices in a BEC cloud by stirring the BEC cloud via rotating external trap potentials [30]. On the other hand, excitation of vortices in BECs, using the optical vortex beams, has been proposed recently using Raman techniques [53–55]. In this section we introduce the scheme, first proposed in Ref. [56] and in Ref. [57], for creation of macroscopic superpositions of vortex-antivortex states through coherent transfer of OAM between laser fields and cold atoms.

Consider an ensemble of condensed atoms with internal five-level M type configuration interacting with four laser beams (Fig. 3). Two strong control lasers respectively drive the transitions $|2\rangle \to |4\rangle$ and $|3\rangle \to |5\rangle$ with Rabi frequencies $\Omega_{c_1} = \Omega_{c_1}^{(0)}\exp(\mathrm{i}\boldsymbol{k}_{c_1}\cdot\boldsymbol{r})$ and $\Omega_{c_2} = \Omega_{c_2}^{(0)}\exp(\mathrm{i}\boldsymbol{k}_{c_2}\cdot\boldsymbol{r})$, where k_{c_j} is the wave-vector. The probe fields, $\Omega_{p_1} = \Omega_{p_1}^{(0)}\mathrm{e}^{\mathrm{i}(l\phi+\boldsymbol{k}_{p_1}\cdot\boldsymbol{r})}$ and $\Omega_{p_2} = \Omega_{p_2}^{(0)}\mathrm{e}^{\mathrm{i}(l'\phi+\boldsymbol{k}_{p_1}\cdot\boldsymbol{r})}$, respectively couple the transitions $|1\rangle \to |4\rangle$ and $|1\rangle \to |5\rangle$ with the wave-vectors $\boldsymbol{k}_{p_j} = k_{p_j}\hat{\boldsymbol{z}} (j=1,2)$. $\Omega_{c_j}^{(0)}$ and $\Omega_{p_j}^{(0)} (j=1,2)$ are the slowly varying amplitudes. Similarly, here we have allowed the two probe photons to have orbital angular momentum $\hbar l$ and $\hbar l'$, respectively. It is convenient to introduce the time-slowly-varying amplitudes $\Psi_2 = \Phi_2\mathrm{e}^{-\mathrm{i}(\omega_{p_1}-\omega_{c_1})t}$, $\Psi_4 = \Phi_4\mathrm{e}^{-\mathrm{i}\omega_{p_1}t}$, $\Psi_3 = \Phi_3\mathrm{e}^{-\mathrm{i}(\omega_{p_2}-\omega_{c_2})t}$, and $\Psi_5 = \Phi_5\mathrm{e}^{-\mathrm{i}\omega_{p_2}t}$. Hence, the equations of motion for the matter fields are given by

$$\begin{aligned}\mathrm{i}\hbar\frac{\partial\Phi_1}{\partial t} &= -\frac{\hbar^2}{2m}\nabla^2\Phi_1 + V_1(\boldsymbol{r})\Phi_1 + (U_{11}|\Phi_1|^2 + U_{12}|\Phi_2|^2 \\ &\quad + U_{13}|\Phi_3|^2)\Phi_1 + \hbar\Omega_{p_1}^*\Psi_4 + \hbar\Omega_{p_2}^*\Phi_5 \end{aligned} \quad (22)$$

$$\begin{aligned}\mathrm{i}\hbar\frac{\partial\Phi_2}{\partial t} &= \left(\epsilon_{12} - \frac{\hbar^2}{2m}\nabla^2\right)\Phi_2 + V_2(\boldsymbol{r})\Phi_2 + (U_{21}|\Phi_1|^2 \\ &\quad + U_{22}|\Phi_2|^2 + U_{32}|\Phi_3|^2)\Phi_1 + \hbar\Omega_{c_1}^*\Phi_4 \end{aligned} \quad (23)$$

$$\begin{aligned}\mathrm{i}\hbar\frac{\partial\Phi_3}{\partial t} &= \left(\epsilon_{13} - \frac{\hbar^2}{2m}\nabla^2\right)\Phi_3 + V_3(\boldsymbol{r})\Phi_3 + (U_{31}|\Phi_1|^2 \\ &\quad + U_{32}|\Phi_2|^2 + U_{33}|\Phi_3|^2)\Phi_1 + \hbar\Omega_{c_2}^*\Phi_5 \end{aligned} \quad (24)$$

$$\begin{aligned}\mathrm{i}\hbar\frac{\partial\Phi_4}{\partial t} &= \left(\epsilon_{14} - \frac{\hbar^2}{2m}\nabla^2\right)\Phi_4 + V_4(\boldsymbol{r})\Phi_4 + \hbar\Omega_{c_1}\Phi_2 \\ &\quad + \hbar\Omega_{p_1}\Phi_1 \end{aligned} \quad (25)$$

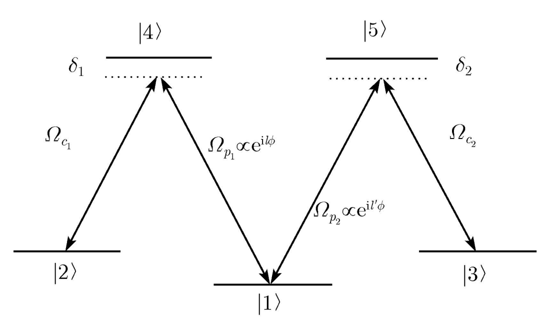

Fig. 3 The five-level M-type scheme for generation of vortex-antivortex states.

$$\mathrm{i}\hbar\frac{\partial\Phi_5}{\partial t}=\left(\epsilon_{15}-\frac{\hbar^2}{2m}\nabla^2\right)\Phi_5+V_5(\boldsymbol{r})\Phi_5+\hbar\Omega_{c_2}\Phi_3+\hbar\Omega_{p_2}\Phi_1 \quad (26)$$

where $V_i(\boldsymbol{r})(i=1,2,3,4,5)$ are the external potentials, the scattering length a_{ij} characterizes the atom-atom interactions via $U_{ij}=4\pi\hbar^2a_{ij}/m$ of which for simplicity we assume the scattering length $a_{ij}=a_0$ is constant. $\epsilon_{14}=\hbar(\omega_{41}-\omega_{p_1})$ and $\epsilon_{15}=\hbar(\omega_{51}-\omega_{p_2})$ are energies of single-photon detunings, while $\epsilon_{12}=\hbar(\omega_{21}-\omega_{p_1}-\omega_{s_1})$ and $\epsilon_{13}=\hbar(\omega_{31}-\omega_{p_2}-\omega_{s_2})$ are energies of the two-photon detunings. To solve the above equations, we shall consider the dark-state condition, i.e., the atoms are approximately restricted on the dark state of the five-level system:

$$|\Psi_D\rangle=\frac{\Omega_{c_1}\Omega_{c_2}}{\Omega_0^2}|1\rangle-\frac{\Omega_{p_1}\Omega_{c_2}}{\Omega_0^2}|2\rangle-\frac{\Omega_{c_1}\Omega_{p_2}}{\Omega_0^2}|3\rangle \quad (27)$$

where $\Omega_0=(|\Omega_{c_1}\Omega_{c_2}|^2+|\Omega_{p_1}\Omega_{c_2}|^2+|\Omega_{c_1}\Omega_{p_2}|^2)^{1/4}$. Since the dark state excludes excited state, the collisions between two excited states and lower states are safely neglected.

It is noteworthy that here our purpose is a little different from that discussed in the former sections. We shall not calculate the adiabatic dynamics of the dark state, but study the dynamics of the coherently generated states Φ_2 and Φ_3. However, since the dark state is not the unitary transformation of the three ground states, generally the dynamics of $\Phi_{2,3}$ cannot solely be determined through Eq. (27) even if we can solve the adiabatic motion of the dark state. To solve this problem, we assume that the two-photon detunings ϵ_{12} and ϵ_{13} are sufficiently small and the strengths of the probe fields are much smaller than that of the control fields, one arrives at the adiabatic Raman passage relating Φ_2 and Φ_3 to Φ_1 [38] through the Eq. (27). In the first order we find

$$\Phi_2=-\xi_1\Phi_1,\quad \Phi_3=-\xi_2\Phi_1 \quad (28)$$

where the ratio coefficients $\xi_1==-\dfrac{\Omega_{p_1}}{\Omega_{c_1}}$ and $\xi_2=-\dfrac{\Omega_{p_2}}{\Omega_{c_2}}$. This result is also the lowest solution of Eqs. (25) and (26). The subsequent derivation for equations of motion for Φ_1,Φ_2 and Φ_3 straightforward. For example, substituting the above relation into the Eqs. (23) and (24), respectively, yields

$$\Phi_4=-(\hbar\Omega_{c_1}^*)^{-1}\left\{\left[\mathrm{i}\hbar\frac{\partial}{\partial t}-\left(\epsilon_{12}-\frac{\hbar^2}{2m}\nabla^2\right)+V_2(\boldsymbol{r})\right]\xi_1^{-1}\Phi_1-(U_{21}|+U_{22}|\xi_1|^{-2}|+U_{32}|\xi_2|^{-2}|)\Phi_1|^2\right\}\Phi_1 \quad (29)$$

$$\Phi_5=-(\hbar\Omega_{c_2}^*)^{-1}\left\{\left[\mathrm{i}\hbar\frac{\partial}{\partial t}-\left(\epsilon_{13}-\frac{\hbar^2}{2m}\nabla^2\right)+V_3(\boldsymbol{r})\right]\xi_2^{-1}\Phi_1+(U_{31}|+U_{32}|\xi_1|^{-2}+U_{33}|\xi_2|^{-2}|)\Phi_1|^2\right\}\Phi_1 \quad (30)$$

Together with the above results, from the Eq. (22) we can obtain the equation of motion for the field Φ_1. Similarly, from the Eq. (22) and Eq. (24) [or Eq. (23)], one can derive the relations between fields $\Phi_{4,5}$ and Φ_2 (or Φ_3), and then substituting them into the Eq. (23) [or Eq. (24)] we can obtain the equation of motion for the field Φ_2 (or Φ_3). Finally, we find the equations of motion for the matter fields Φ_1, Φ_2 and Φ_3 given by

$$\mathrm{i}\hbar\frac{\partial}{\partial t}\Phi_\alpha=\frac{1}{2m}(\mathrm{i}\hbar\nabla+\boldsymbol{A}_\alpha]^2\Phi_\alpha+V_{\alpha\mathrm{eff}}\Phi_\alpha+U|\Phi_1|^2\Phi_\alpha,\quad \alpha=1,2,3 \quad (31)$$

where we have ignored nonlinear terms involving Φ_2 or Φ_3 for small $|\xi_j|$, the nonlinear interaction strength $U=4\pi\hbar^2a_0/m$ and the effective vectors read

$$\boldsymbol{A}_1=\hbar\Xi_1^{-1}(\xi_1^*\nabla\xi_1+\xi_2^*\nabla\xi_2) \quad (32)$$

$$\boldsymbol{A}_2=\hbar\Xi_2^{-1}[1/\xi_2^*\nabla(1/\xi_2)+\xi_1^*/\xi_2^*\nabla(\xi_1/\xi_2)] \quad (33)$$

$$\boldsymbol{A}_3=\hbar\Xi_3^{-1}[1/\xi_1^*\nabla(1/\xi_1)+\xi_2^*/\xi_1^*\nabla(\xi_2/\xi_1)] \quad (34)$$

with $\Xi_1=1+|\xi_1|^2+|\xi_2|^2,\Xi_2=1+1/|\xi_2|^2+|\xi_1|^2/|\xi_2|^2$ and $\Xi_3=1+1/|\xi_1|^2+|\xi_2|^2/|\xi_1|^2$, and the effective trap potentials $V_{1\mathrm{eff}}=\mathrm{i}\hbar\,\Xi_1^{-1}[V_1+|\xi_1|^2V_2+|\xi_2|^2V_3+(2m\Xi_1)^{-1}|\boldsymbol{A}_1|^2], V_{2\mathrm{eff}}=\mathrm{i}\hbar\,\Xi_2^{-1}[V_2+(\epsilon_{21}+V_1)/|\xi_2|^2-V_3|\xi_1|^2/|\xi_2|^2+(2m\Xi_2)^{-1}|\boldsymbol{A}_2|^2]$ and $V_{3\mathrm{eff}}=\mathrm{i}\hbar\,\Xi_3^{-1}[V_3+(\epsilon_{31}+V_1)/|\xi_1|^2-V_2|\xi_2|^2/|\xi_1|^2+(2m\Xi_3)^{-1}|\boldsymbol{A}_3|^2]$. One can find that the effective vectors $\boldsymbol{A}_\alpha(\alpha=1,2,3)$ is generally non-Hermitian, which is easily understood by recalling that $\Phi_{1,2,3}$ are not eigenstates while dark state is. The Hermitian contribution is due to the changes in the phase of $\xi_{1,2}$, while the non-Hermitian part results from the changes of the amplitude of $\xi_{1,2}$. Denoting dimensionless function $\xi_j=\mathrm{e}^{\mathrm{i}R_j}\Omega_{p_j}^{(0)}/\Omega_{c_j}^{(0)}(j=1,2)$ with the phases $R_1=(\boldsymbol{k}_{p_1}-\boldsymbol{k}_{c_1})\cdot\boldsymbol{r}+l\phi$ and $R_2=(\boldsymbol{k}_{p_2}-\boldsymbol{k}_{c_2})\cdot\boldsymbol{r}+l'\phi$, and under the condition $|\nabla|\xi_j|^2|\ll||\xi_j|^2\nabla R_j|$, we can neglect the non-Hermitian part. The effective vectors can then be rewritten as

$$\boldsymbol{A}_1=\hbar\,\Xi_1^{-1}(|\xi_1|^2\nabla R_1+|\xi_2|^2\nabla R_2) \quad (35)$$

$$\boldsymbol{A}_2=-\hbar\,\Xi_2^{-1}(|1/\xi_2|^2\nabla R_2-|\xi_1|^2/|\xi_2|^2\nabla(R_1-R_2)) \quad (36)$$

$$\boldsymbol{A}_3=\hbar\Xi_3^{-1}(|1/\xi_1|^2\nabla R_1-|\xi_2|^2/|\xi_1|^2\nabla(R_2-R_1)) \quad (37)$$

When $|\xi_1|^2=|\xi_2|^2$, i.e., the ratio between the Rabi frequencies $\Omega_{p_1}^{(0)}$ and $\Omega_{c_1}^{(0)}$ equals that between $\Omega_{p_2}^{(0)}$ and

$\Omega_{c_2}^{(0)}$, and the photons of two input probe fields have opposite orbital angular momentum, i.e. $l = -l'$, it is easy to verify $\boldsymbol{A}_1 = 0$ and $\boldsymbol{A}_2 = -\boldsymbol{A}_3 = \boldsymbol{A} = -\hbar l \nabla \phi$. The Eqs. (31) can be recast into

$$\mathrm{i}\hbar \frac{\partial}{\partial t}\begin{pmatrix}\Phi_2\\ \Phi_3\end{pmatrix} = \frac{1}{2m}(\mathrm{i}\hbar\nabla + q\sigma_3 \boldsymbol{A})^2 \begin{pmatrix}\Phi_2\\ \Phi_3\end{pmatrix} + \begin{pmatrix}V_{2\mathrm{eff}} & 0\\ 0 & V_{3\mathrm{eff}}\end{pmatrix} \cdot \begin{pmatrix}\Phi_2\\ \Phi_3\end{pmatrix} + U|\Phi_1|^2 \begin{pmatrix}\Phi_2\\ \Phi_3\end{pmatrix} \quad (38)$$

where σ_3 is the pauli matrix, $q = +1$, and

$$\mathrm{i}\hbar \frac{\partial}{\partial t}\Phi_1 = -\frac{1}{2m}\hbar\nabla^2\Phi_1 + V_{1\mathrm{eff}}(\boldsymbol{r})\Phi_1 \quad (39)$$

The results (38) and (39) can be interpreted as that the three categories of condensates with effective electric charges $q_1 = 0$ and $q_2 = -q_3 = q = +1$, respectively, interact with an effective $U(1)$ gauge field $\boldsymbol{A}$. In other words, by employing two probe lights that respectively have orbital angular momentum $\pm l\hbar$ in the $\pm z$ direction, we obtain an effective two-flavor (oppositely charged) condensate which has attracted special attention in recent years [59, 60]. Alternatively, if we call Φ_2 and Φ_3 as (pseudo-)spin up $|\uparrow\rangle$ and down $|\downarrow\rangle$ state, the above result can be understood that different spin states experience opposite effective gauge fields. For the present purpose, since $|\xi_j|^2 \ll 1$, the small depletion of atoms in state $|1\rangle$ can be neglected, and then Eq. (38) is linearized by putting $|\Phi_1| \approx \sqrt{\rho(\boldsymbol{r})}$ with $\rho(\boldsymbol{r})$ the total density of the condensate. In this way, the lowest order solution of Eq. (38) is given by

$$\Phi_2(\boldsymbol{r},t) = -\frac{\Omega_{p_1}^{(0)}}{\Omega_{c_1}^{(0)}}\sqrt{\rho(\boldsymbol{r})}\exp\left[\mathrm{i}S_2(\boldsymbol{r},t)\right] \quad (40)$$

$$\Phi_3(\boldsymbol{r},t) = -\frac{\Omega_{p_2}^{(0)}}{\Omega_{c_2}^{(0)}}\sqrt{\rho(\boldsymbol{r})}\exp\left[\mathrm{i}S_3(\boldsymbol{r},t)\right] \quad (41)$$

where the phases $S_2(\boldsymbol{r},t) = \frac{q_2}{\hbar}\int_0^{\boldsymbol{r}} \boldsymbol{A}\cdot \mathrm{d}\boldsymbol{r}' + S_{02}(\boldsymbol{r},t)$ and $S_3(\boldsymbol{r},t) = \frac{q_3}{\hbar}\int_0^{\boldsymbol{r}} \boldsymbol{A}\cdot \mathrm{d}\boldsymbol{r}' + S_{03}(\boldsymbol{r},t)$ with $S_{02}(\boldsymbol{r},t) = \bar{\boldsymbol{k}}_2\cdot\boldsymbol{r} - \int_0^t \mathrm{d}t'\{V_{2\mathrm{eff}}[\boldsymbol{r} + \bar{\boldsymbol{K}}_2(t'-t)] + U\rho[\boldsymbol{r} + \bar{\boldsymbol{K}}_2(t'-t)]\}$ and $S_{03}(\boldsymbol{r},t) = \bar{\boldsymbol{k}}_3\cdot\boldsymbol{r} - \int_0^t \mathrm{d}t'\{V_{3\mathrm{eff}}\,[\boldsymbol{r} + \bar{\boldsymbol{K}}_3(t'-t)] + U\rho[\boldsymbol{r} + \bar{\boldsymbol{K}}_3(t'-t)]\}$. $\bar{\boldsymbol{K}}_2 = \hbar\bar{\boldsymbol{k}}_2/m = \hbar(\boldsymbol{k}_{p_1} - \boldsymbol{k}_{c_1})/m$ and $\bar{\boldsymbol{K}}_3 = \hbar\bar{\boldsymbol{k}}_3/m = \hbar(\boldsymbol{k}_{p_2} - \boldsymbol{k}_{c_2})/m$ are the corresponding recoil velocities. The velocity spread of the two generated BECs can be obtained as $\boldsymbol{v}_j(\boldsymbol{r}) = \hbar\nabla_{\boldsymbol{r}} S_j(\boldsymbol{r},t)/m$ $(j = 2,3)$. By a straightforward calculation one can verify that the loop integration of the velocity yields $\oint_{z=0\in C_j} \boldsymbol{v}_j(\boldsymbol{r}')\cdot \mathrm{d}\boldsymbol{r}' = \pm 2\pi\hbar l/m$ $(j = 2,3)$, where the sign of right-hand side of the above equation takes + (for $j = 2$) or − (for $j = 3$). $z = 0 \in C_j$ means that the integration path C_j encircles the z-axis. The above results indicate that the orbital angular momenta of input probe fields are fully transferred into the generated BECs Φ_2 and Φ_3.

A simple but interesting application of the above results is that if the input probe lights are the components of a superposition of opposite OAM states (vortex qubits): $|+l\rangle \pm |-l\rangle$, we can obtain the macroscopic superposition of vortex-antivortex states for the matter fields through the above coherent transfer technique of vortex states. Creation of a general superposition of the OAM states of light has been studied in Ref. [57], and the created vortex qubits for BECs are supposed to have interesting fundamental and practical applications [58].

5 Spin Hall effect in atoms

Spin hall effect (SHE) has recently attracted much attention since its prediction in solid systems with spin-orbit coupled structures [61−66], with the concomitant creation of spin currents and study of quantized spin hall conductance. The physics of SHE in semiconductors can be understood in the following way: In the presence of spin-orbit coupling, the applied electric field leads to a transverse motion (perpendicular to the electric field) of spins, with the spin-up and spin-down carriers transporting opposite to each other; thus, a spin current is created perpendicular to the electric field. Quantized SHE was predicted in metallic graphene [67, 68], mercury telluride-cadmium telluride semiconductor systems [69] and in semiconductors with a strain gradient structure [70]. In the latter cases, quantum SHE is essentially the phenomenon in which particles in different spin directions experience opposite effective gauge fields formed through spin-orbit couplings, resulting in a non-vanishing quantized spin hall conductance and a vanishing charge hall conductance.

According to the discussion in the former sections, we know the effective gauge field on atoms can be readily generated through atom-light couplings. Properly adjusting the parameters of external laser fields, one can reach the situation that different atomic spin states (angular-momentum states) experience opposite gauge fields, leading to SHE in atomic systems. Such an idea was first proposed in Refs. [50] and [51].

Figure 4 shows the level configuration of an ensemble of cold Fermi atoms interacting with two external light fields. The ground $\left(|g_\pm, \pm\frac{1}{2}\rangle\right)$ and excited $\left(|e_\pm, \pm\frac{1}{2}\rangle\right)$ states are hyperfine angular momentum states (atomic spins) with their total angular momenta $F_g = F_e = 1/2$.

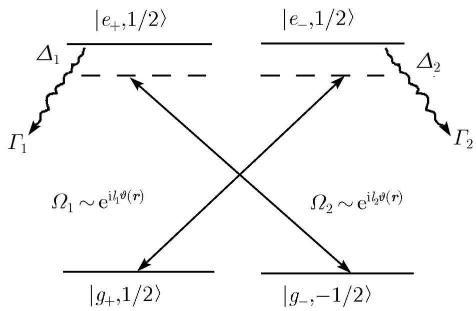

Fig. 4 Fermi atoms with four-level internal hyperfine spin states interacting with two light fields. This can be experimentally realized with alkali atoms, such as ^{6}Li atoms ($2^2S_{1/2}(F=1/2) \longleftrightarrow 2^2P_{1/2}(F'=1/2)$) [71, 72].

The laser fields are characterized by the Rabi-frequencies $\Omega_1 = \Omega_{10}\exp[i(\boldsymbol{k}_1 \cdot \boldsymbol{r} + l_1\vartheta)]$ and $\Omega_2 = \Omega_{20}\exp[i(\boldsymbol{k}_2 \cdot \boldsymbol{r} + l_2\vartheta)]$. Here, the phase $\vartheta = \arctan(y/x)$. For simplicity, in the following discussion we replace the notations $|\alpha_\pm, \pm\frac{1}{2}\rangle$ by $|\alpha_\pm\rangle$ ($\alpha = e, g$). The $\boldsymbol{r}$-representation atomic wave function is denoted by $\Phi_\alpha(\boldsymbol{r}, t)$. Similar to former discussions, we introduce the slowly-varying amplitudes of atomic wave-functions by (setting $\omega_{g\pm} = 0$): $\Psi_{g_\pm} = \Phi_{g_\pm}$, $\Psi_{e_+} = \Phi_{e_+}(\boldsymbol{r}, t)e^{-i[\boldsymbol{k}_2 \cdot \boldsymbol{r} - (\omega_{e_+} - \Delta_1)t]}$, $\Psi_{e_-} = \Phi_{e_-}(\boldsymbol{r}, t)e^{-i[\boldsymbol{k}_1 \cdot \boldsymbol{r} - (\omega_{e_-} - \Delta_2)t]}$, where $\hbar\omega_\alpha$ is the energy of the state $|\alpha\rangle$, Δ_1 and Δ_2 are respectively the detuning of σ_+ and σ_- light fields. The Hamiltonian of the present system can be written as $H = H_0 + H_1 + H_2$, where

$$H_0 = \sum_{\alpha = e_\pm g_\pm} \int d^3r\, \Psi_\alpha^* \left[-\frac{\hbar^2}{2m}\nabla^2 + V(\boldsymbol{r})\right] \Psi_\alpha$$

$$H_1 = \hbar\Delta_1 \int d^3r\, \Psi_{e_+}^* S_{e_+e_+} \Psi_{e_+} + \hbar \int d^3r (\Psi_{e_+}^* \Omega_{10} e^{il_1\vartheta} S_{1+} \Psi_{g_-} + h.a.) \tag{42}$$

$$H_2 = \hbar\Delta_2 \int d^3r\, \Psi_{e_-}^* S_{e_-e_-} \Psi_{e_-} + \hbar \int d^3r (\Psi_{e_-}^* \Omega_{20} e^{il_2\vartheta} S_{2+} \Psi_{g_+} + h.a.)$$

with atomic operators $S_{e_\pm e_\pm} = |e_\pm\rangle\langle e_\pm|$, $S_{1+} = |e_+\rangle\langle g_-|, S_{2+} = |e_-\rangle\langle g_+|$, $S_{1+}^\dagger = S_{1-}$ and $S_{2+}^\dagger = S_{2-}$. $V(\boldsymbol{r})$ is the external trap potential. The collisions (s-wave scattering) between cold Fermi atoms are negligible. The interaction part of the Hamiltonian can be diagonalized with the following local unitary transformation:

$$U(\boldsymbol{r}) = \begin{pmatrix} U_1 & 0 \\ 0 & U_2 \end{pmatrix} \tag{43}$$

with

$$U_j = \begin{pmatrix} \cos\theta_j & \sin\theta_j e^{il_j\vartheta(\boldsymbol{r})} \\ -\sin\theta_j e^{-il_j\vartheta(\boldsymbol{r})} & \cos\theta_j \end{pmatrix}, \quad j = 1, 2$$

Under this transformation, the four eigenstates of interaction Hamiltonian can be obtained as $\left[|\psi_+\rangle, |\psi_-\rangle\right]^T = U_1\left[|e_+\rangle, |g_-\rangle\right]^T$ and $\left[|\phi_+\rangle, |\phi_-\rangle\right]^T = U_2\left[|e_-\rangle, |g_+\rangle\right]^T$. The mixing angles θ_j are defined according to $\tan\theta_1 = E_\psi^-/E_\psi^+$ and $\tan\theta_2 = E_\phi^-/E_\phi^+$, where the eigenvalues of $|\psi_\pm\rangle$ and $|\phi_\pm\rangle$ can be calculated by: $E_\psi^\pm = (\Delta_1 \pm \sqrt{\Delta_1^2 + 4\Omega_{10}^2})/2$ and $E_\phi^\pm = (\Delta_2 \pm \sqrt{\Delta_2^2 + 4\Omega_{20}^2})/2$.

In order to suppress the spontaneous emission of the excited states, we shall consider the large detuning case, i.e. $\Delta_j^2 \gg \Omega_{j0}^2$. By calculating all values up to the order of Ω_{j0}^2/Δ_j^2, one can verify that $\tan\theta_j = \Omega_{j0}/\Delta_j$, and $E_{\psi,\phi}^+ \gg E_{\psi,\phi}^-$. According to the Eq. (9), atomic motion may lead to the transitions between ground eigenstates and excited ones. For example, the element of transition between $|\psi_+\rangle$ and $\psi_-\rangle$ can be calculated by

$$\tau_\pm = |\langle\psi_+|\partial_t|\psi_-\rangle| \sim |\bar{\boldsymbol{v}}_f \cdot \nabla\theta_1(\boldsymbol{r}) + \frac{1}{2}\sin 2\theta_1 \bar{\boldsymbol{v}}_f \cdot \nabla\vartheta_1(\boldsymbol{r})| \tag{44}$$

where $\bar{\boldsymbol{v}}_f$ is the fermi velocity of the atomic system. For our purpose we require $\tau_\pm \ll |E_\psi^+ - E_\psi^-|$ so that the coupling between ground states and excited states can be neglected. Then, we introduce the adiabatic condition that the population of the higher levels $|\psi_+\rangle$ and $|\phi_+\rangle$ is adiabatically eliminated, say, meanwhile the total system is restricted to the ground eigenstates

$$|\Psi\rangle = \cos\gamma|\psi_-\rangle + \sin\gamma|\phi_-\rangle = \cos\gamma|S_\downarrow\rangle + \sin\gamma|S_\uparrow\rangle \tag{45}$$

where, to facilitate further discussions, we have put the effective spin states: $|S_\downarrow\rangle = |\psi_-\rangle$, $|S_\uparrow\rangle = |\phi_-\rangle$ with their z-component effective spin polarizations $S_z^\uparrow = \frac{\hbar}{2}(\cos^2\theta_2 - \sin^2\theta_2) \approx \hbar/2$ and $S_z^\downarrow = \frac{\hbar}{2}(\sin^2\theta_1 - \cos^2\theta_1) \approx -\hbar/2$. The parameter γ describes the possibility of an atom in states $|S_\downarrow\rangle$ and $|S_\uparrow\rangle$, and can be determined by the initial condition. It is easy to see that the probability of excited states is much smaller than that of the ground states for $|S_{\uparrow,\downarrow}\rangle$ ($\sin^2\theta_j \ll \cos^2\theta_j$), therefore the atomic decay can be safely neglected in the present situation.

Under the above adiabatic condition, the local transformation $U(\boldsymbol{r})$ can lead to a diagonalized $SU(2)$ gauge potential:

$$\frac{e}{c}\begin{pmatrix} \boldsymbol{A}_\downarrow & 0 \\ 0 & \boldsymbol{A}_\uparrow \end{pmatrix} = i\hbar\begin{pmatrix} \langle S_\downarrow|\nabla|S_\downarrow\rangle & 0 \\ 0 & \langle S_\uparrow|\nabla|S_\uparrow\rangle \end{pmatrix} \tag{46}$$

where $e > 0$ is the positive effective charge of an atom and c is the vacuum light speed. Accordingly, the effective (scalar) trap potentials read $V_\alpha(\boldsymbol{r}) = V(\boldsymbol{r}) - \hbar|\Delta_j|^{-1}\Omega_{j0}^2 - (2m)^{-1}|\hbar\langle S_\alpha|\nabla|S_\alpha\rangle|^2$ with $j = 1$ (for $\alpha =\downarrow$) and $j = 2$ (for $\alpha =\uparrow$). Especially, we have

$$\boldsymbol{A}_\downarrow = -\boldsymbol{A}_\uparrow = \hbar lce^{-1}\frac{\Omega_0^2}{\Delta^2}(x\hat{e}_y - y\hat{e}_x)/\rho^2 \tag{47}$$

and

$$V_{\text{eff}}(\boldsymbol{r}) = V_{\uparrow,\downarrow}(\boldsymbol{r}) = V(\boldsymbol{r}) - \hbar\Omega_0^2/\Delta - \frac{\hbar^2 l^2 \Omega_0^4}{(2m\Delta^4\rho^2)} \tag{48}$$

with $\rho = \sqrt{x^2+y^2}$, when we choose $\Delta_1 = \Delta_2 = \Delta$, $\Omega_{10} = \Omega_{20} = \Omega_0$ and $l_1 = -l_2 = l$, i.e., the angular momenta of the two light fields are opposite in direction. This result is intrinsically interesting: by coupling the atomic spin states to radiation, we find the atomic system can be described as an ensemble of charged particles with opposite spins experiencing opposite magnetic fields but the same electric field. With the help of gauge and trap potentials, we can rewrite the Hamiltonian in the following effective form:

$$\begin{aligned} H = &\int \mathrm{d}^3r\, \Psi_{s_\downarrow}^* \left[\frac{1}{2m}\left(\hbar\partial_k + \mathrm{i}\frac{e}{c}A_k\right)^2\right] \Psi_{s_\downarrow} \\ &+ \int \mathrm{d}^3r\, \Psi_{s_\uparrow}^* \left[\frac{1}{2m}\left(\hbar\partial_k - \mathrm{i}\frac{e}{c}A_k\right)^2\right] \Psi_{s_\uparrow} \\ &+ \int \mathrm{d}^3r (V_\downarrow|\Psi_{s_\downarrow}|^2 + V_\uparrow|\Psi_{s_\uparrow}|^2) \end{aligned} \tag{49}$$

where $\Psi_{s_\downarrow}(\boldsymbol{r}) = \cos\gamma\langle\boldsymbol{r}|S_\downarrow\rangle$ and $\Psi_{s_\uparrow}(\boldsymbol{r}) = \sin\gamma\langle\boldsymbol{r}|S_\uparrow\rangle$ are spin wave functions in $\boldsymbol{r}$-representation.

The spin current in the present system has several important properties. First, it satisfies the conservation law. The spin density in the present system is calculated according to

$$\boldsymbol{S}(\boldsymbol{r},t) = \Psi_{s_\downarrow}^* \boldsymbol{S}_\downarrow \Psi_{s_\downarrow} + \Psi_{s_\uparrow}^* \boldsymbol{S}_\uparrow \Psi_{s_\uparrow} \tag{50}$$

with $\boldsymbol{S}_{\uparrow\downarrow} = (S_x^{\uparrow\downarrow}, S_y^{\uparrow\downarrow}, S_z^{\uparrow\downarrow})$. On the other hand, the spin current density $\boldsymbol{J}_k(\boldsymbol{r},t) = (J_k^{s_x}, J_k^{s_y}, J_k^{s_z})$ is defined by

$$\begin{aligned} \boldsymbol{J}_k = &-\frac{\mathrm{i}\hbar}{m}\boldsymbol{S}_\downarrow(\Psi_{s_\downarrow}^* D_{1k}\Psi_{s_\downarrow} - \Psi_{s_\downarrow} D_{1k}^* \Psi_{s_\downarrow}^*) \\ &-\frac{\mathrm{i}\hbar}{m} S_\uparrow(\Psi_{s_\uparrow}^* D_{2k}\Psi_{s_\uparrow} - \Psi_{s_\uparrow} D_{2k}^* \Psi_{s_\uparrow}^*) \end{aligned} \tag{51}$$

where $D_{1k} = \partial_k + \mathrm{i}\frac{e}{c}A_k$ and $D_{2k} = \partial_k - \mathrm{i}\frac{e}{c}A_k$ are the covariant derivative operators. By a straightforward calculation we can verify the following continuity equation:

$$\partial_t \boldsymbol{S}(\boldsymbol{r},t) + \partial_k \boldsymbol{J}_k = A_k\sigma_z\hat{\boldsymbol{e}}_z \times \boldsymbol{J}_k(\boldsymbol{r},t) \tag{52}$$

where σ_z is the pauli matrix. It is easy to see for the s_z-component spin current, that the right hand side of Eq. (52) equals zero. Thus, the spin current $J_k^{s_z}$ is conserved. Note that there is no spin-orbit coupling in the present atomic system and that it can be verified that the orbit-angular momentum current is also conserved. These results confirm the conservation law for s_z-component of total angular momentum current of atoms. Second, the spin current in the present system may exhibit interesting topological properties. For convenience, we denote

$$\Psi_{s_\alpha} = \sqrt{2m}\eta\zeta_\alpha, \quad \alpha =\uparrow,\downarrow \tag{53}$$

where the complex $\zeta_\alpha = |\zeta_\alpha|\mathrm{e}^{-\mathrm{i}\varphi_\alpha}$ with $|\zeta_\downarrow|^2 + |\zeta_\uparrow|^2 = 1$. The modulus η is related to the total atomic density which is assumed to be constant in our case. Then the s_z-component of Eq. (51) can be recast into

$$\begin{aligned} J_k^{s_z} &= -\mathrm{i}\hbar^2\eta^2(\zeta_\downarrow\partial_k\zeta_\downarrow^* - \zeta_\downarrow^*\partial_k\zeta_\downarrow + \zeta_\uparrow^*\partial_k\zeta_\uparrow - \zeta_\uparrow\partial_k\zeta_\uparrow^*) \\ &\quad -2\hbar^2\eta^2\frac{e}{c}A_k \\ &= \hbar^2\eta^2[\partial_k(\varphi_1 - \varphi_2) - (|\zeta_\downarrow|^2 - |\zeta_\uparrow|^2)\partial_k(\varphi_1+\varphi_2)] \\ &\quad -2\hbar^2\eta^2\frac{e}{c}A_k \end{aligned} \tag{54}$$

Furthermore, we introduce the unit vector field by $\boldsymbol{\lambda} = (\bar{\zeta}, \boldsymbol{\sigma}\zeta)$, where $\zeta = (\zeta_\downarrow, \zeta_\uparrow^*)^{\mathrm{T}}$ and $\boldsymbol{\sigma} = (\sigma_x, \sigma_y, \sigma_z)$. It then follows that $\lambda_1 = \zeta_\downarrow^*\zeta_\uparrow^* + \zeta_\downarrow\zeta_\uparrow, \lambda_2 = \mathrm{i}(\zeta_\downarrow\zeta_\uparrow - \zeta_\downarrow^*\zeta_\uparrow^*)$ and $\lambda_3 = |\zeta_\downarrow|^2 - |\zeta_\uparrow|^2$. Based on these variables we can finally find the following result:

$$(\nabla\times\boldsymbol{J}^{s_z})_m = -2\hbar^2\eta^2\frac{e}{c}B_m - \frac{1}{2}\hbar^2\eta^2\epsilon_{mkl}\boldsymbol{\lambda}\cdot(\partial_k\boldsymbol{\lambda}\times\partial_l\boldsymbol{\lambda}) \tag{55}$$

The contribution $\boldsymbol{\lambda}\cdot(\partial_k\boldsymbol{\lambda}\times\partial_l\boldsymbol{\lambda})$ indicates a topological term in the spin current induced by optical fields. Note each value of $\boldsymbol{\lambda}$ represents a point in the two-dimensional sphere S^2. The variation of $\boldsymbol{\lambda}$ depends on the relative density of the two spin components $\gamma(\boldsymbol{r})$ and the sum of the phase spreadings $\varphi_\uparrow(\boldsymbol{r}) + \varphi_\downarrow(\boldsymbol{r})$. It is easy to verify that $\boldsymbol{\lambda}$ can cover the entire surface S^2 for the parameter distributions in the interaction region: $\varphi_1 + \varphi_2 : 0 \to 2n_1\pi$ and $\gamma : 0 \to n_2\pi/2$ with integers $n_1, n_2 \geqslant 1$. We then obtain a map between the unit vector field $\boldsymbol{\lambda}$ and the spatial vectors $F : \boldsymbol{\lambda} \to \boldsymbol{r}/r$ so that the closed-surface integral

$$\oint_s (\nabla\times\boldsymbol{J}^{s_z})\cdot\mathrm{d}\boldsymbol{S} \sim \oint_s \mathrm{d}s_m\epsilon_{mkl}\frac{\boldsymbol{r}}{r}\cdot\left(\partial_k\frac{\boldsymbol{r}}{r}\times\partial_l\frac{\boldsymbol{r}}{r}\right) \sim 4\pi n$$

where n is the winding number. In physics, such mapping degree corresponds to the formation of a local inhomogeneity in the densities of the spin-up and spin-down atoms. The Hamiltonian (49) can also be understood as a system with *two-flavor* oppositely charged particles interacting with *one* external effective magnetic field. Such model has a wide range of application in, e.g. twoband superconductivity [73, 74], etc. For instance, under certain conditions liquid metallic hydrogen might allow for the coexistence of superconductivity with both electronic and protonic Cooper pairs [75]. Faddeev *et al.* have discovered a series of nontrivial topological properties in these systems [59, 60]. Again, based on our technique, we develop an optical way to realize a *two-flavor* artificially charged system, which may allow for a deeper understanding of the basic physical mechanisms in cold atomic systems.

For practical application, an important goal is to create a pure spin current injection, i.e., there is no accompanying massive current. For this we use two columnar spreading light fields that [43, 44] $\Omega_{01}(\boldsymbol{r}) = \Omega_{02}(\boldsymbol{r}) = f\rho$ with $f > 0$. Furthermore, we set the potential $V(\boldsymbol{r}) = \frac{1}{2}\nu(\boldsymbol{\rho} + x_0\hat{\boldsymbol{e}}_x)^2$ with the coefficient $\nu = \left(1 + \frac{\hbar l^2 f^2}{2m\Delta^3}\right)\frac{2\hbar f^2}{\Delta}$, say, we use a two-dimensional harmonic potential centered at $\boldsymbol{\rho} = -x_0\hat{\boldsymbol{e}}_x$ [76]. Then we reach a set of uniform magnetic field

$$\boldsymbol{B}_{\downarrow}(-\boldsymbol{B}_{\uparrow}) = \frac{\hbar lc}{e}\frac{f^2}{\Delta^2}\hat{e}_z \tag{56}$$

and electric fields

$$\boldsymbol{E} = -\nabla V_{\text{eff}}(\boldsymbol{r}) = -\left(1 + \frac{\hbar l^2 f^2}{4m\Delta^3}\right)\frac{2\hbar f^2 x_0}{e\Delta}\hat{e}_x \tag{57}$$

respectively in z $(-z)$ and x directions. Atoms in different spin states $|S_\alpha\rangle$ experience the opposite magnetic fields $\boldsymbol{B}_\alpha$ but the same electric field $\boldsymbol{E}$. This may lead to a Landau level structure for each spin orientation. Together with the applied in-plane electric field, one can obtain a pure spin current in the y direction, while the massive current is zero. To exactly calculate the spin currents, we need to calculate the eigenstates of the present system. The Hamiltonian for a single atom in state $|S_\alpha\rangle$ can be written as:

$$H^\alpha = H_0^\alpha + H', \quad \alpha = \downarrow, \uparrow$$
$$H' = -eEx$$
$$H_0^\alpha = \frac{\hbar^2 eB}{2mc}(R_\alpha^2 + P_\alpha^2) + \frac{1}{2m}p_z^2 \tag{58}$$

with $R_{\uparrow\downarrow} = \left(\frac{c}{eB}\right)^{1/2}\left(p_x - \frac{e}{c}A_x^{\uparrow\downarrow}\right), P_{\uparrow\downarrow} = \left(\frac{c}{eB}\right)^{1/2}\left(p_y - \frac{e}{c}A_y^{\uparrow\downarrow}\right)$ and $B = |\boldsymbol{B}_{\uparrow,\downarrow}|$. One can verify that $[R_\alpha, P_\beta] = \mathrm{i}\hbar\delta_{\alpha\beta}$, so the eigenfunction of H_0^α is Hermite polynomial, written as $\mu_{nk}^\alpha(R)$ with the Landau level $E_{nk,\alpha} = (n + 1/2)\hbar\omega + \hbar k^2/2m$ and $\omega = eB/mc$. In the weak field case, the spin/massive current carried by an atom can be calculated to the first-order correction with perturbation theory on the state $|\mu_{nk}^\alpha\rangle$ (linear response)

$$(j_{s_z,m}^y)_{nk,\alpha} = \langle\mu_{nk}^\alpha|j_{s_z,m}^y|\mu_{nk}^\alpha\rangle + \Big(\sum_{n'\alpha'}\frac{\langle\mu_{n'k}^{\alpha'}|H'|\mu_{nk}^\alpha\rangle\langle\mu_{nk}^\alpha|j_{s_z,m}^y|\mu_{n'k}^{\alpha'}\rangle}{E_{n,\alpha} - E_{n',\alpha'}} + h.a.\Big) \tag{59}$$

where the spin current operator is

$$(j_{s_z}^y)_\alpha = \frac{\hbar}{2}(S_z^\alpha v_y^\alpha + v_y^\alpha S_z^\alpha) \tag{60}$$

with $v_y^\alpha = [y, H^\alpha]/\mathrm{i}h = (eB/m^2c)^{1/2}P_\alpha$ and the massive current operator $j_m = mv_y$. The two terms in the right hand side of the above equation respectively refer to the zeroth and first-order correction. It is easy to see that $\langle\mu_{nk}^\alpha|j_{s_z,m}^y|\mu_{n'k}^{\alpha'}\rangle = 0$ when $n' \neq n \pm 1$, thus only the terms with $n' = n \pm 1$ contribute to the above equation.

If the space-spreading lengths of the atoms in x and z directions are L_x and L_z, respectively, the average current density for the total system is given by

$$J_{s_z,m}^y = \frac{1}{L_x L_z}\int \mathrm{d}E[(j_{s_z,m}^{(0)})_{nk,\alpha} + (j_{s_z,m}^{(1)})_{nk,\alpha}]f(E) \tag{61}$$

with $f(E)$ the Fermi distribution function. For ^{6}Li atoms we consider the initial condition that $\sin^2\gamma = \cos^2\gamma = 1/2$, i.e., the atoms have the equal possibility in state $|S_\downarrow\rangle$ and $|S_\uparrow\rangle$, which is familiar in optical traps [77]. Note that under the present definitions the perturbation part can be rewritten as $H' = \mathrm{i}\hbar E\left(\frac{ec}{B}\right)^{1/2}\frac{\partial}{\partial R}$. Substituting this result into Eqs. (60) and (61) we get

$$J_{s_z}^y = n_a\left(\hbar + \frac{\hbar^2 l^2 f^2}{4m\Delta^3}\right)\frac{\Delta x_0}{l} \tag{62}$$

where $n_a = 2m\eta^2$ is the density of atoms, whereas the massive current $J_m = 0$. In fact, under the present interaction of external effective electric and magnetic fields, the atoms with opposite velocities in y direction have opposite spin polarizations (see Fig. 5). Thus, the massive current vanishes whereas a pure spin current is obtained. This result allows us to create conserved spin currents without using atomic beams.

To observe SHE in present cold atomic systems, a spin-sensitive measurement [78] can be used. After the spin current is created, the spin-up and spin-down atoms will respectively accumulate in opposite sides along the y direction of the atom chip. Experimentally, one can detect such spatially separated spin accumulation via, e.g. fluorescence measurement. For ^{6}Li atoms, one could perform resonant Raman transitions from the accumulated spin

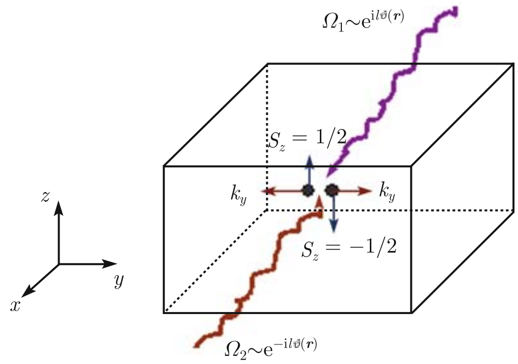

Fig. 5 Under the interaction of effective electric and magnetic fields induced by light fields, atoms in state $|S_\downarrow\rangle$ ($S_z = -1/2$) and $|S_\uparrow\rangle$ ($S_z = 1/2$) have opposite momenta in the y direction.

state $S_z = -1/2$ to $2^2\mathrm{P}_{1/2}(F = 3/2, m = -3/2)$ and from $S_z = 1/2$ to $2^2\mathrm{P}_{1/2}(F = 3/2, m = 3/2)$ and then observe fluorescence. As long as the spin accumulations are separated to, e.g., larger than $5-10$ microns, the two separated images can be resolved in the experiment.

Finally, we can numerically check the adiabatic condition in the present system. The typical values of the parameters can be set $\Delta \sim 10^7\mathrm{s}^{-1}, l < 10^4, f = 10^{7-8}(\mathrm{s}\cdot\mathrm{m})^{-1}, x_0 \approx 0.2$ mm. The velocity then satisfies $\bar{v} < 1.0$ m/s and $\tau_\pm/|E^+_\psi - E^-_\psi| < 10^{-3} \ll 1$, which guarantees the validity of the adiabatic condition. Furthermore, if we employ an atomic system with the atomic density $n_a \approx 1.0 \times 10^{10}\mathrm{cm}^{-3}$, one can find the spin current $J^y_{s_z} \approx 1.322 \times 10^{-5}\mathrm{eV/cm}^2$. On the other hand, practically the light fields have a finite cross section S_{xy}, whose effect is ignored in the calculation of spin currents. For our purpose, this effect can be neglected when $lf^2S_{xy}/\Delta^2 \gg 1$, which means the effective magnetic flux induced by the light fields can support an enough large number of quantum states for each Landau level. Since the decoherence rate of atomic spin currents is generally much smaller than that of the counterparts in semiconductors, the created atomic spin currents could be applicable in quantum information devices.

6 Discussion and conclusions

Generation of adiabatic gauge field in the cold atomic system is a rapidly developing research field in recent years. The adiabatic gauge field in atomic systems, which leads to effective spin-orbit couplings in atomic motion, can result in very rich physical features. Compared with the solid system, where the spin-orbit coupling is originated from Dirac equation, the effective spin-orbit coupling in atomic systems is created via atom-light coupling, and has more freedom in controllability, and thus attracts wide attention. Besides the results discussed in this work, several interesting applications of the adiabatic gauge field in cold atoms have been investigated. For example, By extending the atomic SHE from fermi systems to bosonic systems, the fractional spin Hall effect (FSHE) can be studied [79]. Generalized Stern-Gerlach effect is studied by extending the result in three-level Λ-type atomic systems to Δ-type systems [80]. In the four-level tripod atomic system, the effective Rashba and linear Dresselhaus model is obtained by properly adjusting the atom-light interactions [81]. Combining the approach of creating non-Abelian gauge field with optical lattice, many interesting results can be obtained, e.g. realization of the non-Abelian Aharonov-Bohm effect, non-Abelian interferometry and simulating lattice gauge dynamics [82].

In summary, we have reviewed the general theory of generating adiabatic gauge field in quantum systems and in particular, we have discussed how to generate effective spin-orbit couplings in atomic systems by coupling atoms to external optical fields with OAM. Two novel applications of the adiabatic gauge field in atoms have been studied. First, we introduced the scheme for the creation of macroscopic superposition of vortex-antivortex states from a five-level M-type atomic system, and then we showed the realization of the spin Hall effect in fermi atomic system. Further investigations on the applications of the adiabatic gauge field in atoms and experimental demonstration of the theoretically predicted results will be the next focus in this intriguing topic.

Acknowledgements This work was supported by NUS (National University of Singapore) academic research under the grant No. WBS: R-144-000-189-305, US NSF (Natural Science Foundation) under the grant No. DMR-0547875.

References

1. A. S. Parkins, P. Marte, P. Zoller, and H. J. Kimble, Phys. Rev. Lett.,1993, 71: 3095
2. T. Pelizzari, S. A. Gardiner, J. I. Cirac, and P. Zoller, Phys. Rev. Lett., 1995, 75: 3788
3. J. I. Cirac, P. Zoller, H. J. Kimble, and H. Mabuchi, Phys. Rev. Lett., 1997, 78: 3221
4. N. V. Vitanov, M. Fleischhauer, B. W. Shore, and K. Bergmann, Adv. At. Mol., Opt. Phys., 2001, 46: 55
5. H. J. Kimble, Phys. Scr., 1998, 76: 127
6. S. E. Harris, J. E. Field, and A. Kasapi, Phys. Rev. A, 1992, 46: R29
7. M. O. Scully and M. S. Zubairy, Quantum Optics, Cambridge: Cambridge University Press, 1999
8. L. V. Hau, S. E. Harris, Z. Dutton, and C. H. Behroozi, Nature (London), 1999, 397: 594

9. M. Fleischhauer and M. D. Lukin, Phys. Rev. Lett., 2000, 84: 5094
10. M. Fleischhauer and M. D. Lukin, Phys. Rev. A, 2002, 65: 022314
11. C. Liu, Z. Dutton, C. H. Behroozi, and L. V. Hau, Nature (London), 2001, 409: 490
12. D. F. Phillips, A. Fleischhauer, A. Mair, R. L. Walsworth, and M. D. Lukin, Phys. Rev. Lett., 2001, 86: 783
13. M. Fleischhauer and S. Q. Gong, Phys. Rev. Lett., 2002, 88: 070404
14. L. M. Kuang and L. Zhou, Phys. Rev. A, 2003, 68: 043606
15. Y. Wu, J. Saldana and Y. Zhu, Phys. Rev. A, 2003, 67: 013811
16. Y. Wu and L. Deng, Phys. Rev. Lett., 2004, 93: 143904
17. Y. Wu, M. G. Payne, E. W. Hagley, and L. Deng, Phys. Rev. A, 2004, 70: 063812
18. Y. Wu, Phys. Rev. A, 2005, 71: 053820
19. C. P. Sun, Y. Li, and X. F. Liu, Phys. Rev. Lett., 2003, 91: 147903
20. X. J. Liu, H. Jing, and M. L. Ge, Phys. Rev. A, 2004, 70: 055802
21. X. J. Liu, H. Jing, X. Liu, and M. L. Ge, Phys. Lett. A, 2006, 355: 437
22. X. J. Liu, X. Liu, Z. X. Liu, L. C. Kwek, and C. H. Oh, Phys. Rev. A, 2007, 75: 023809
23. A. André, L.-M. Duan, and M. D. Lukin, Phys. Rev. Lett., 2002, 88: 243602
24. D. Matsukevich and A. Kuzmich, Science, 2004, 306: 663
25. B. Julsgaard, J. Sherson, J. I. Cirac, J. A. Fiurasek, and E. S. Polzik, Nature (London), 2004, 432: 482
26. B. B. Blinov, D. L. Moehring, L. M. Duan, and C. Monroe, Nature (London), 2004, 428: 153
27. D. N. Matsukevich, T. Chaneliere, M. Bhattacharya, S. Y. Lan, S. D. Jenkins, T. A. B. Kennedy, and A. Kuzmich, Phys. Rev. Lett., 2005, 95: 040405
28. W. Rosenfeld, S. Berner, J. Volz, M. Weber, and H. We. Infurter, Phys. Rev. Lett., 2007, 98: 050504
29. M. Lewenstein, A. Sanpera, V. Ahufinger, B. Damski, A. Sen De, and U. Sen, Adv. Phys., 2007, 56: 243
30. P. Engels, I. Coddington, P. C. Haljan, and E. A. Cornell, Phys. Rev. Lett., 2002, 89: 100403
31. B. Paredes, P. Fedichev, J. I. Cirac, and P. Zoller, Phys. Rev. Lett., 2001, 87: 010402
32. B. Paredes, P. Fedichev, J. I. Cirac, and P. Zoller, Phys. Rev. A, 2002, 66: 033609
33. J. R. Abo-Shaeer, C. Raman, J. M. Vogels, and W. Ketterle, Science, 2001, 292: 476
34. T. L. Ho, Phys. Rev. Lett., 2001, 87: 060403
35. U. R. Fischer and G. Baym, Phys. Rev. Lett., 2003, 90: 140402
36. A. S. Søensen, E. Demler, and M. D. Lukin, Phys. Rev. Lett., 2005, 94: 086803
37. A. A. Abrikosov, Sov. Phys. JETP, 1957, 5: 1174
38. G. Juzeliunas and P. Ohberg, Phys. Rev. Lett., 2004, 93: 033602
39. D. Jaksch and P. Zoller, New J. Phys., 2003, 5: 56
40. G. Juzeliunas, P. Ohberg, J. Ruseckas, and A. Klein, Phys. Rev. A, 2005, 71: 053614
41. J. Ruseckas, G. Juzeliunas, P. Ohberg, and M. Fleischhauer, Phys. Rev. Lett., 2005, 95: 010404
42. M. T. Gabriel, P. Tores Juan, and T. Lluis, Nature Physics, 2007, 3: 305
43. L. Allen, S. M. Barnett and M. J. Padgett, Optical Angular Momentum, Bristol: Institute of Physics, 2003
44. E. M. Wright, J. Arlt, and K. DhoLaKia, Phys. Rev. A, 2001, 63: 013608
45. L. Allen, M. J. Padgett, and M. Babiker, Prog. Opt., 1999, 39: 291
46. M. S. Soskin and M. V. Vasnetsov, Prog. Opt., 2001, 42: 219
47. F. Wilczek and A. Zee, Phys. Rev. Lett., 1984, 52: 2111
48. K. G. Wilson, Phys. Rev. D, 1974, 10: 2445
49. C. P. Sun and M. L. Ge, Phys. Rev. D, 1990, 41: 1349
50. X.-J. Liu, X. Liu, L. C. Kwek, and C. H. Oh, Phys. Rev. Lett., 2007, 98: 026602, arXiv: cond-mat/0603083
51. S.-L. Zhu, H. Fu, C.-J. Wu, S.-C. Zhang, and L.-M. Duan, Phys. Rev. Lett., 2006, 97: 240401
52. M. R. Matthews, B. P. Anderson, P. C. Haljan, D. S. Hall, C. E. Wieman, and E. A. Cornell, Phys. Rev. Lett., 1999, 83: 2498
53. K.-P. Marzlin, W. Zhang, and E. M. Wright, Phys. Rev. Lett., 1997, 79: 4728
54. G. Nandi, R. Walser, and W. P. Schleich, Phys. Rev. A, 2004, 69: 063606
55. Z. Dutton and J. Ruostekoski, Phys. Rev. Lett., 2004, 93: 193602
56. X.-J. Liu, H. Jing, X. Liu, and M.-L. Ge, Eur. Phys. J. D, 2006, 37: 261
57. K. T. Kapale1 and J. P. Dowling, Phys. Rev. Lett., 2005, 95: 173601
58. M. Liu, L. H. Wen, H. W. Xiong, and M. S. Zhan, Phys. Rev. A, 2006, 73: 063620
59. L. Faddeev and A. J. Niemi, Phys. Rev. Lett., 2000, 85: 3416
60. E. Babaev, L. D. Faddeev, and A. J. Niemi, Phys. Rev. B, 2002, 65: 100512
61. S. Murakami, N. Nagaosa, and S.-C. Zhang, Science, 2003, 301: 1348
62. J. Sinova, D. Culcer, Q. Niu, N. A. Sinitsyn, T. Jungwirth, and A. H. MacDonald, Phys. Rev. Lett., 2004, 92: 126603
63. Y. K. Kato, R. C. Myers, A. C. Gossard, and D. D. Awschalom, Science, 2004, 306: 1910
64. J. Wunderlich, B. Kaestner, J. Sinova, and T. Jungwirth, Phys. Rev. Lett., 2005, 94: 047204
65. B. K. Nikolic, S. Souma, L. P. Zârbo, and J. Sinova, Phys. Rev. Lett., 2005, 95: 046601
66. S. Murakami, N. Nagaosa, and S.-C. Zhang, Phys. Rev. Lett., 2004, 93: 156804
67. C. L. Kane and E. J. Mele, Phys. Rev. Lett., 2005, 95: 226801

68. N. A. Sinitsyn, J. E. Hill, Hongki Min, J. Sinova, and A. H. MacDonald, arXiv: cond-mat/0602598
69. B. A. Bernevig, Taylor L. Hughes, and S.-C. Zhang, Science, 2006, 314: 1757
70. B. A. Bernevig and S.-C. Zhang, Phys. Rev. Lett., 2006, 96: 106802
71. B. DeMarco and D. S. Jin, Science, 1999, 285: 1703
72. M. E. Gehm, Preparation of an Optically-trapped Degenerate Fermi Gas of ^{6}Li: Finding the Route to Degeneracy, Doctor Thesis, Duke University, 2003
73. L. Shen, N. Senozan, and N. Phillips, Phys. Rev. Lett., 1965, 14: 1025
74. F. Bouquet, R. A. Fisher, N. E. Phillips, D. G. Hinks, and J. D. Jorgensen, Phys. Rev. Lett., 2001, 87: 047001
75. K. Moulopoulos and N. W. Ashcroft, Phys. Rev. B, 1999, 59: 12309
76. R. Grimm and M. Weidemuller, Optical Dipole Traps for Neutral Atoms, In: Advances in Atomic, Molecular and Optical Physics, 2000, Vol. 42: 95
77. Z. Hadzibabic, S. Gupta, C. A. Stan, C. H. Schunck, M. W. Zwierlein, K. Dieckmann, and W. Ketterle, Phys. Rev. Lett., 2003, 91: 160401
78. Artem M. Dudarev, Roberto B. Diener, Iacopo Carusotto, and Q. Niu, Phys. Rev. Lett., 2004, 92: 153005
79. X.-J. Liu, X. Liu, L. C. Kwek, and C. H. Oh, arXiv: cond-mat/0701506
80. Y. Li, C. Bruder, and C. P. Sun, Phys. Rev. Lett., 2007, 99: 130403
81. T. D. Stanescu, C. W. Zhang, and V. Galitski, Phys. Rev. Lett., 2007, 99: 110403
82. K. Osterloh, M. Baig, L. Santos, P. Zoller, and M. Lewenstein, Phys. Rev. Lett., 2005, 95: 010403